POSTBUCKLING RESPONSE OF LONG THICK PLATES LOADED IN COMPRESSION INCLUDING HIGHER ORDER TRANSVERSE SHEARING EFFECTS

Manuel Stein* and P. Daniel Sydow
Structural Mechanics Division
NASA Langley Research Center

Liviu Librescu
Department of Engineering Science and Mechanics
Virginia Polytechnic Institute and State University

Abstract

This paper presents buckling and postbuckling results for compression-loaded simply-supported aluminum plates and composite plates with a symmetric lay-up of thin ±45° plies composed of many layers. Buckling results for aluminum plates of finite length are given for various length-to-width ratios. Asymptotes to the curves based on the buckling results give N_{xcr} for plates of infinite length. Postbuckling results for plates with transverse shearing flexibility are compared to results from classical theory for various width-to-thickness ratios. Characteristic curves indicating the average longitudinal direct stress resultant as a function of the applied displacements are calculated based on four different theories: classical von Karman theory using the Kirchhoff assumptions, first-order shear deformation theory, higher-order shear deformation theory, and three-dimensional flexibility theory. Present results indicate that the three-dimensional flexibility theory gives the lowest buckling loads. The higher-order shear deformation theory has fewer unknowns than the three-dimensional flexibility theory but does not take into account through-the-thickness effects. The figures presented show that small differences occur in the average longitudinal direct stress resultants from the four theories that are functions of applied end-shortening displacement.

Nomenclature

A_{11}, A_{12}, A_{22}, A_{33}, A_{44}, A_{55}, A_{66}	Plate extensional stiffnesses
a, b, h	Dimensions of the rectangular plate parallel to x, y, and z axes, respectively
C_{11}, C_{12}, C_{22}, C_{33}, C_{44}, C_{55}, C_{66}	Stiffnesses used in Hooke's Law
D_{11}, D_{12}, D_{22}, D_{66}	Plate bending stiffnesses
E	Young's modulus
H_{44}, I_{44}, J_{12}, J_{22}, J_{66}, K_{12}, K_{22}, K_{66}	Plate stiffness components, defined in equation (A14) in the Appendix
L_x, L_y, L_z, L_{yz}, L_{xz}, L_{xy}, M_x, M_y, M_{xy}	Moment resultants in the plate
N_x, N_y, N_{xy}	Inplane stress resultants in the plate
N_{yz}, N_{xz}	Transverse stress resultants in the plate
N_{xav}	Average compressive load per unit length
N_{xcr}	Value of N_{xav} at buckling
Q, Q_y	Functions of y defined in Appendix
U	Applied end shortening
U_{cr}	Value of U at buckling
u, v, w	Displacements in x, y, and z directions, respectively
x, y, z	Plate coordinates
β_1, β_2	Functions of y defined in Appendix
ε_x, ε_y, ε_z, γ_{yz}, γ_{xz}, γ_{xy}	Strains in the plate
λ	Buckle half-wavelength
μ	Poisson's ratio
σ_x, σ_y, σ_z, τ_{yz}, τ_{xz}, τ_{xy}	Stresses in the plate

*Senior Aerospace Engineer, Associate Fellow, AIAA

Introduction

The increasing interest in minimum weight designs for aeronautical and aerospace structures has generated substantial interest in the analysis of the elastic stability and postbuckling behavior of structures subjected to inplane compressive loads. For thin homogeneous plates, classical plate theory predicts deformations and inplane stresses that are comparable to those of three-dimensional elasticity. Transverse stresses in thin plates are generally small compared to inplane stresses, and thus, both classical theory and first-order shear deformation theory give satisfactory results. However, since both theories are two-dimensional, they are not accurate enough to predict transverse stresses directly. Accurate nonlinear theories are required for the analysis of thick plates in which these transverse stresses become more significant.

It is often sufficient to use an accurate nonlinear two-dimensional theory to solve some three-dimensional nonlinear elasticity problems. However, when through-the-thickness effects become more dominant, it is important to use a nonlinear theory that takes into account such effects. One such theory has been derived in reference 1 for laminated and thick plates with three-dimensional flexibility effects. This theory can predict directly the transverse stresses as well as the inplane stresses by using trigonometric terms in addition to the usual constant and linear terms representing through-the-thickness variation of the displacements. However, this theory cannot satisfy the surface boundary conditions of a plate.

The purpose of the present paper is to present the results of an investigation of the buckling and postbuckling response of orthotropic plates loaded in compression. Classical nonlinear von Karman theory using the Kirchhoff assumptions and three nonlinear transverse shearing theories are used to predict results for different values of plate width-to-thickness ratios in the postbuckling range. The nonlinear transverse shearing theories are: first-order shear deformation theory, references 2 and 3; higher-order shear deformation theory, reference 4; and three-dimensional flexibility theory, reference 1. The idea of satisfying exactly the static tangential or surface boundary conditions on the external planes of the plate (or shell) was used in references 5, 6, and 7. The first papers dealing with postbuckling where the static tangential or surface boundary conditions on the external planes of the plate were satisfied are references 8 and 9. The present derivation of the higher-order shear deformation theory has the advantage of having nonlinear through-the-thickness terms without contributing additional unknowns to the first-order shear deformation theory. In addition, it satisfies the surface boundary conditions of the plate. The essential difference between the higher-order shear deformation theory and the three-dimensional flexibility theory is that the higher-order shear deformation theory is a two-dimensional theory that uses cubic terms, whereas the three-dimensional flexibility theory is a three-dimensional theory that uses trigonometric terms in addition to the constant and linear terms that represent the through-the-thickness variation of the inplane displacements. The paper presents the derivation of the nonlinear plate equations for buckling of plates loaded in axial compression for both higher-order theories. This paper also presents postbuckling results for the average longitudinal compressive direct stress resultant and maximum stress resultants as a function of the applied displacements, and maximum out-of-plane displacement as a function of the applied end-shortening displacement. The plates considered in this paper are infinitely long with side edges simply supported and are loaded in uniaxial compressive end shortening. The side edges are free to slide along the edges to allow constant longitudinal strain. Results for the four theories are presented for

aluminum plates and for composite plates with a symmetric lay-up composed of many layers of thin ±45° plies.

Theory

A brief outline of the derivation of the four different theories compared in this paper is presented in this section. The derivation of equations using classical von Karman-Kirchhoff theory has been presented in reference 9. The derivation of equations using first-order shear deformation theory has been presented in references 2 and 3. The derivation of the equations for the two higher-order theories are not given in detail elsewhere, so they are presented in the appendix. The general approach used in deriving the equations to be solved is the same as in reference 10. First, the displacement functions for each theory are identified. Then the nonlinear strain-displacement relations are written to include the assumption that the displacements are sinusoidal along the length of the infinitely long plate. Stress-strain relations are defined for a "specially orthotropic" plate. Application of the principle of virtual work leads to ordinary differential equations and variationally consistent boundary conditions which are solved using a procedure based on Newton's method as discussed in reference 11.
The displacements considered for each theory are:

Classical von Karman-Kirchhoff theory

$$\begin{aligned} u(x,y,z) &= u^{o}(x,y) - w^{o}_{,x}(x,y)\frac{z}{h} \\ v(x,y,z) &= v^{o}(x,y) - w^{o}_{,y}(x,y)\frac{z}{h} \\ w(x,y,z) &= w^{o}(x,y) \end{aligned} \tag{1}$$

First-order shear deformation theory

$$\begin{aligned} u(x,y,z) &= u^{o}(x,y) + u^{a}(x,y)\frac{z}{h} \\ v(x,y,z) &= v^{o}(x,y) + v^{a}(x,y)\frac{z}{h} \\ w(x,y,z) &= w^{o}(x,y) \end{aligned} \tag{2}$$

Higher-order shear deformation theory

$$u(x,y,z) = u^{o}(x,y) + \left[u^{a}(x,y) - \frac{4h}{3}\left(\frac{u^{a}(x,y)}{h} + w^{o}_{,x}(x,y)\right)\left(\frac{z}{h}\right)^{2}\right]\frac{z}{h}$$

$$v(x,y,z) = v^{o}(x,y) + \left[v^{a}(x,y) - \frac{4h}{3}\left(\frac{v^{a}(x,y)}{h} + w^{o}_{,y}(x,y)\right)\left(\frac{z}{h}\right)^{2}\right]\frac{z}{h} \tag{3}$$

$$w(x,y,z) = w^{o}(x,y)$$

Three-dimensional flexibility theory

$$\begin{aligned} u(x,y,z) &= u^{o}(x,y) + u^{a}(x,y)\frac{z}{h} + u^{s}(x,y)\sin\frac{\pi z}{h} \\ v(x,y,z) &= v^{o}(x,y) + v^{a}(x,y)\frac{z}{h} + v^{s}(x,y)\sin\frac{\pi z}{h} \\ w(x,y,z) &= w^{o}(x,y) + w^{c}(x,y)\cos\frac{\pi z}{h} \end{aligned} \tag{4}$$

In this paper the zero subscripts correspond to the constant-in-z terms, the a superscripts correspond to the algebraic-in-z terms, and the s and c superscripts correspond to the trigonometric-in-z terms.

Both the classical von Karman-Kirchhoff and the first-order shear deformation theories have inplane deformations u and v which are linear in z. Classical theory, however, has the additional assumption that there is zero transverse shearing ($\gamma_{xz} = \gamma_{yz} = 0$), thus eliminating u^a and v^a in favor of derivatives of w^o.

The higher-order shear deformation theory considers inplane deformations u and v which are cubic in z. As explained in reference 10, the squared-in-z term vanishes and the cubic term does not introduce any new variables beyond those that appear in first-order shear deformation theory if the boundary conditions are satisfied at $z = \pm h/2$. The three-dimensional flexibility theory considers trigonometric terms in u, v, and w beyond the expressions considered for the deformations of first-order shear deformation theory.

To account for the applied displacement U,

$$\begin{aligned} u^{o}(x,y) &= -U\frac{x}{a} + U^{o}_{2}(x,y) \\ v^{o}(x,y) &= v^{o}_{o}(y) + V^{o}_{2}(x,y) \end{aligned} \tag{5}$$

To satisfy the assumption that the displacements are sinusoidal along the length

$$\begin{aligned} U^{o}_{2} &= u^{o}_{2}(y)\sin\frac{2\pi x}{\lambda} \\ V^{o}_{2} &= v^{o}_{2}(y)\cos\frac{2\pi x}{\lambda} \end{aligned} \tag{6}$$

All the other u coefficients can be expressed as functions of y multiplied by $\cos \pi x/\lambda$, where λ is the half-wavelength of the buckled plate. All the other v and w coefficients can be expressed as functions of y multiplied by $\sin \pi x/\lambda$. The strain-displacement relations used are

$$\begin{aligned} \varepsilon_x &= u_{,x} + \frac{1}{2}w_{,x}^{2} \\ \varepsilon_y &= v_{,y} + \frac{1}{2}w_{,y}^{2} \\ \varepsilon_z &= w_{,z} \\ \gamma_{yz} &= v_{,z} + w_{,y} \\ \gamma_{xz} &= u_{,z} + w_{,x} \\ \gamma_{xy} &= u_{,y} + v_{,x} + w_{,x}w_{,y} \end{aligned} \tag{7}$$

Hooke's law that relates stresses to strains for a "specially orthotropic" plate is used here

$$\begin{vmatrix} \sigma_x \\ \sigma_y \\ \sigma_z \\ \tau_{yz} \\ \tau_{xz} \\ \tau_{xy} \end{vmatrix} = \begin{bmatrix} C_{11} & C_{12} & 0 & 0 & 0 & 0 \\ C_{12} & C_{22} & 0 & 0 & 0 & 0 \\ 0 & 0 & C_{33} & 0 & 0 & 0 \\ 0 & 0 & 0 & C_{44} & 0 & 0 \\ 0 & 0 & 0 & 0 & C_{55} & 0 \\ 0 & 0 & 0 & 0 & 0 & C_{66} \end{bmatrix} \begin{vmatrix} \varepsilon_x \\ \varepsilon_y \\ \varepsilon_z \\ \gamma_{yz} \\ \gamma_{xz} \\ \gamma_{xy} \end{vmatrix} \tag{8}$$

Ordinary differential equations and variationally consistent boundary conditions are derived using the principle of virtual work, and the equations are solved by Newton's method. The principle of virtual work applied to the internal forces of a three-dimensional body considered here is

$$\delta\Pi = \int_0^a \int_0^b \int_{-h/2}^{h/2} (\sigma_x\delta\varepsilon_x + \sigma_y\delta\varepsilon_y + \sigma_z\delta\varepsilon_z + \tau_{xy}\delta\gamma_{xy} + \tau_{xz}\delta\gamma_{xz} + \tau_{yz}\delta\gamma_{yz})\,dz\,dy\,dx \tag{9}$$

with simple support boundary conditions at y = 0 and y = b.

The half-wavelength λ of the assumed deformations for the infinitely long plates considered is chosen to minimize the buckling load for each given applied deformation.

The principle of virtual work requires that the geometric boundary conditions be satisfied. Including additional terms in the representation of the through-the-thickness variation of the inplane displacements will lead to convergence and satisfaction of natural boundary conditions in the limit if a complete set of terms is used. An alternate approach is to use terms that satisfy the natural boundary conditions directly. A complete set of these terms also leads to convergence. For the present problem, the three-dimensional flexibility theory uses terms that do not satisfy the natural boundary conditions. For the higher-order shear deformation theory, coefficients of u and v in the assumed displacements of equation (3) are chosen such that $\gamma_{xz} = 0$ and $\gamma_{yz} = 0$. The coefficients are written in terms of the existing unknowns u^a, v^a, and w^o in a form which satisfies the natural boundary conditions at the top and bottom surfaces of the plate. Comparisons of results are valid whether or not natural boundary conditions are satisfied.

Results and Discussion

The results obtained in this study for long aluminum plates with the geometry shown in figure 1 are based on values of Young's modulus $E = 10.7 \times 10^6$ psi and Poisson's ratio $\mu = .33$. The results obtained in this study for infinitely long composite plates with a symmetric lay-up composed of many layers of thin ±45° plies are based on the stiffness properties

$A_{11} = A_{22} = 620340$ lb/in. $A_{12} = 446060$ lb/in. $A_{33} = 59000$ lb/in.
$A_{44} = A_{55} = 50000$ lb/in. $A_{66} = 483520$ lb/in.
$D_{11} = D_{22} = 518.6$ lb in. $D_{12} = 372.91$ lb in. $D_{66} = 404.23$ lb-in.

for h = .1 in. and for any value of b.

Buckling results given by the four theories are presented in figure 2 for finite aluminum plates and the results show the variation of the buckling stress coefficient with width-to-thickness ratio b/h for a range of length-to-width ratios a/b. Asymptotes to the curves in figure 2 give N_{xcr} for plates of infinite length. The differences in the buckling results for aluminum plates with width-to-thickness ratios less than ten, illustrate the need for including the effects of transverse shear deformations when determining the compressive buckling stress of these plates.

Results in the form of average axial stress resultant $N_{x_{av}}$ versus applied end-shortening U, for the four theories and different values of the width-to-thickness ratio b/h, are presented in figures 3a and 3b for aluminum plates and composite plates, respectively. In figure 3a, only one curve is shown for a b/h value of 100 since the corresponding results for each theory are approximately the same. Even for the thicker aluminum plates there are only slight differences in the results given by the different theories. The results presented in figure 3b illustrate the nature of the more compliant ±45° composite plate. The more pronounced separation in the postbuckling branches of the curves for a given value of the b/h ratio indicates the reduction in transverse shear stiffness in the composite plates.

The results show that the higher-order shear deformation theory gives a better approximation of the effects of shear deformation in thick plates than the first-order theory, but it is still a two-dimensional theory. Significant improvement beyond that already obtained with the higher-order theory requires a three-dimensional theory. The three-dimensional flexibility theory is an attempt to meet this requirement. However, the present formulation of this three-dimensional theory has limitations associated with the assumptions made on the w displacement of equation (A10). Although it does include a trigonometric term in z, this term does not satisfy the bounding conditions at the upper and lower surfaces of the plates, and therefore does not allow σ_z to have its proper influence on w. Additionally, the assumption that the nonlinear terms involving w^c could be neglected because they were small in comparison to similar terms involving only w^o may be questionable. A secondary effect is the choice of the specially orthotropic material which foregoes the influence of ε_z on σ_y. Neither of these two effects becomes significant until the effects of shear deformation become more dominant. Evidence of these limitations are especially noticeable for results of the three-dimensional flexibility theory at a b/h value of 20 in figures 4b, 5b, and 6b.

The results presented in figures 4a and 4b for the aluminum and composite plates show that the higher-order shear deformation theory gives the lowest value of normalized compressive N_{ymax} for higher values of normalized end-shortening U. In figure 4b, the results for the three-dimensional flexibility theory at a b/h value of 20 exhibit nonlinear behavior in the postbuckling range. These results suggest an increase in the importance of the unsatisfied bounding conditions at the upper and lower surfaces of the plate. Similar behavior for the three-dimensional flexibility theory at a b/h value of 20 is shown in figures 5b and 6b.

The results presented in figure 5a show that the normalized N_{xymax} as a function of normalized end-shortening U is nearly independent of the width-to-thickness ratio b/h for the aluminum plates, whereas figure 5b shows that the effect of the width-to-thickness ratio b/h is more significant for the composite plates. Results for the normalized maximum deflection w_{max} presented as a function of normalized end-shortening U in figures 6a and 6b, for aluminum plates and composite plates respectively, show that the value of the deflection becomes increasingly dependent upon the width-to-thickness ratio b/h as the value of the normalized end-shortening U increases. These results indicate that shear deformation effects are more dominant for the composite plates, especially at lower values of the width-to-thickness ratio b/h.

Present results indicate that three-dimensional flexibility theory gives lower buckling loads than the other theories, and produces acceptable results except when the effect of the missing nonlinear terms involving w^c and the influence of the bounding conditions become dominant. The three-dimensional flexibility theory has the potential for permitting the development of a rigorous approach for obtaining direct through-the-thickness stress components without the current limitations caused by using additional trigonometric terms in z in the expansion of the transverse displacement w and by retaining the currently neglected nonlinear terms involving w^c. Higher-order shear deformation theory has the advantage of fewer unknowns than the three-dimensional theory and yet it gives comparable results to those given by three-dimensional flexibility theory. For the ±45° composite plates, results show more pronounced nonlinear behavior in the postbuckling range as the plate width-to-thickness ratio b/h decreases. This more pronounced nonlinear response is a direct result of the increase in shear flexibility of the more compliant ±45° composite plates. The difference in the order of the approximation of the four theories is most evident for the ±45° composite plate results, particularly for the average axial stress resultant $N_{x_{av}}$ as a function of the applied displacement U, and for the maximum out-of-plane displacement w as a function of the applied displacement U.

Concluding Remarks

This paper presents buckling and postbuckling results for aluminum plates and ±45° composite plates subjected to longitudinal compressive end-shortening displacements. The side edges of the plates are simply supported and free to slide along the edges to allow constant longitudinal strain. The effects of varying plate width and thickness on the buckling stress coefficient is described. The buckling results for aluminum plates with width-to-thickness ratios less than ten, indicate that including the effects of transverse shear deformation is important when determining the compressive buckling stress and these effects should be included. Postbuckling results for plates with transverse shearing flexibility are compared to results from classical theory for various width-to-thickness ratios. Characteristic curves indicating the average longitudinal direct stress resultant as a function of the applied displacements are calculated based on four different theories: classical von Karman theory, a first-order shear deformation theory, a higher-order shear deformation theory that satisfies the bounding conditions at the upper and lower

surfaces of the plate, and a three-dimensional flexibility theory that can predict the transverse and inplane stresses directly.

Present results indicate that the three-dimensional flexibility theory gives the lowest buckling loads for the four theories considered, and produces acceptable results except when the effect of the missing nonlinear terms involving the coefficient w^c of the trigonometric term in the expansion of the transverse displacement w and the influence of the bounding conditions becomes dominant. The three-dimensional flexibility theory has the potential for permitting the development of a rigorous approach for obtaining direct through-the-thickness stress components without the current limitations caused by using additional trigonometric terms in z in the expansion of the transverse displacement w and by retaining the currently neglected nonlinear terms involving w^c. The higher-order shear deformation theory has fewer unknowns than the three-dimensional flexibility theory but cannot predict transverse or inplane stresses. The figures presented show that, for postbuckling of aluminum plates, small differences occur in the average longitudinal direct stress resultant, in the maximum values of the other stress resultants, and in the maximum transverse displacements calculated when the effects of transverse shear flexibility are included in the various theories. For the ±45° composite plates, results show more pronounced nonlinear behavior in the postbuckling range as the plate width-to-thickness ratio b/h decreases. This more pronounced nonlinear response is a direct result of the increase in shear flexibility of the more compliant ±45° composite plates. The difference in the order of the approximation of the four theories is most evident for the ±45° composite plates results, particularly for the results for the average axial stress resultant $N_{x_{av}}$ as a function of the applied displacement U, and for the maximum out-of-plane displacement w as a function of the applied displacement U.

Appendix

Governing differential equations are derived in more detail in this appendix for the two higher-order theories considered in this paper.

Higher-order shear deformation theory

The displacements used in this theory are given by equations (3) as

$$u(x,y,z) = u^o(x,y) + \left[u^a(x,y) - \frac{4h}{3}\left(\frac{u^a(x,y)}{h} + w^o_{,x}(x,y)\right)\left(\frac{z}{h}\right)^2\right]\frac{z}{h}$$

$$v(x,y,z) = v^o(x,y) + \left[v^a(x,y) - \frac{4h}{3}\left(\frac{v^a(x,y)}{h} + w^o_{,y}(x,y)\right)\left(\frac{z}{h}\right)^2\right]\frac{z}{h} \qquad \text{(A1)}$$

$$w(x,y,z) = w^o(x,y)$$

Substitution of equations (3) into equation (7) gives the strain-displacement relations

$$\varepsilon_x = u^o_{,x} + \frac{1}{2}w^{o\,2}_{,x} + u^a_{,x}\frac{z}{h} - \frac{4}{3}\left(\frac{z}{h}\right)^3\left(u^a_{,x} + w^o_{,xx}h\right)$$

$$\varepsilon_y = v^o_{,y} + \frac{1}{2}w^{o\,2}_{,y} + v^a_{,y}\frac{z}{h} - \frac{4}{3}\left(\frac{z}{h}\right)^3\left(v^a_{,y} + w^o_{,yy}h\right)$$

$$\gamma_{xy} = u^o_{,y} + v^o_{,x} + w^o_{,x}w^o_{,y} + \left(u^a_{,y} + v^a_{,x}\right)\frac{z}{h} - \frac{4}{3}\left(\frac{z}{h}\right)^3\left(u^a_{,y} + v^a_{,x} + 2w^o_{,xy}h\right) \qquad \text{(A2)}$$

$$\gamma_{xz} = \left(w^o_{,x} + \frac{u^a}{h}\right)\left(1 - \left(\frac{2z}{h}\right)^2\right)$$

$$\gamma_{yz} = \left(w^o_{,y} + \frac{v^a}{h}\right)\left(1 - \left(\frac{2z}{h}\right)^2\right)$$

The assumption that the displacements are sinusoidal along the length leads to

$$u^o = -U\frac{x}{a} + u^o_2(y)\sin\frac{2\pi x}{\lambda} \qquad v^o = v^o_0(y) + v^o_2(y)\cos\frac{2\pi x}{\lambda}$$

$$u^a = u^a_1(y)\cos\frac{\pi x}{\lambda} \qquad v^a = v^a_1(y)\sin\frac{\pi x}{\lambda} \qquad \text{(A3)}$$

$$w^o = w^o_1(y)\sin\frac{\pi x}{\lambda}$$

Stresses are determined from Hooke's law according to equation (8), and stress resultant forces and moments are determined by the following integrals through the thickness

$$N_{x_o} + N_{x_2}\cos\frac{2\pi x}{\lambda} = \int_{-h/2}^{h/2}\sigma_x dz$$

$$N_{y_o} + N_{y_2}\sin\frac{2\pi x}{\lambda} = \int_{-h/2}^{h/2}\sigma_y dz$$

$$N_{yz_o}\sin\frac{\pi x}{\lambda} = \int_{-h/2}^{h/2}\tau_{yz}\left(1 - \frac{4z^2}{h^2}\right)dz$$

$$N_{xz_o}\cos\frac{\pi x}{\lambda} = \int_{-h/2}^{h/2}\tau_{xz}\left(1 - \frac{4z^2}{h^2}\right)dz \qquad \text{(A4)}$$

$$N_{xy_2}\sin\frac{2\pi x}{\lambda} = \int_{-h/2}^{h/2}\tau_{xy}dz$$

$$M_{x_o}\sin\frac{\pi x}{\lambda} = \int_{-h/2}^{h/2}\sigma_x z\,dz$$

$$M_{x_1}\sin\frac{\pi x}{\lambda} = \int_{-h/2}^{h/2} -\frac{4}{3}h\sigma_x\left(\frac{z}{h}\right)^3 dz$$

$$M_{y_o}\sin\frac{\pi x}{\lambda} = \int_{-h/2}^{h/2}\sigma_y z\,dz$$

$$M_{y_1}\sin\frac{\pi x}{\lambda} = \int_{-h/2}^{h/2} -\frac{4}{3}h\sigma_y\left(\frac{z}{h}\right)^3 dz$$

$$M_{xy_o}\cos\frac{\pi x}{\lambda} = \int_{-h/2}^{h/2}\tau_{xy}z\,dz$$

$$M_{xy_1}\cos\frac{\pi x}{\lambda} = \int_{-h/2}^{h/2} -\frac{4}{3}h\tau_{xy}\left(\frac{z}{h}\right)^3 dz$$

Substitution of the stresses and strains into the virtual work expression, equation (9), and performing the variation leads to the differential equations

$$u_2^{o\prime} = \frac{2\pi}{\lambda} v_2^o - \frac{1}{2} w_1^o \beta_2 \frac{\pi}{\lambda} + \frac{N_{xy_2}}{A_{66}}$$

$$v_2^{o\prime} = \frac{1}{4}\beta_2^2 - \frac{A_{12}}{A_{22}}\left(u_2^o \frac{2\pi}{\lambda} + \frac{1}{4} w_1^{o\,2} \left(\frac{\pi}{\lambda}\right)^2\right) + \frac{N_{y_2}}{A_{22}} \qquad \text{(A5)}$$

$$\frac{u_1^{a\prime}}{h} = -\frac{v_1^a}{h}\frac{\pi}{\lambda} + \left(M_{xy_1} - (\bar{D}_{66} + \bar{B}_{66})\frac{2\pi}{\lambda}\beta_2\right) \Big/ \left(D_{66} + 2\bar{D}_{66} + \bar{B}_{66}\right)$$

$$\frac{v_1^{a\prime}}{h} = \left[\bar{B}_{22}\left(M_{y_o} - M_{y_1}\right) - \bar{D}_{22} M_{y_1} + \left(D_{12}\bar{B}_{22} - \bar{D}_{12}\bar{D}_{22}\right)\frac{u_1^a}{h}\frac{\pi}{\lambda} + \left(\bar{D}_{12}\bar{B}_{22} - \bar{B}_{12}\bar{D}_{22}\right)\left(u_1^a \frac{\pi}{\lambda} + w_1^o \left(\frac{\pi}{\lambda}\right)^2\right)\right] \Big/ \left(D_{22}\bar{B}_{22} - \bar{D}_{22}^2\right)$$

$$v_o^{o\prime} = -\frac{1}{4}\beta_2^2 - \frac{A_{12}}{A_{22}}\left(-U + \frac{1}{4} w_1^{o\,2}\left(\frac{\pi}{\lambda}\right)^2\right) + \frac{N_{y_o}}{A_{22}}$$

$$N_{xy_2}' = \frac{2\pi}{\lambda} N_{x_2}$$

$$N_{y_2}' = -\frac{2\pi}{\lambda} N_{xy_2}$$

$$M_{xy_1}' = -\frac{\pi}{\lambda}\left(M_{x_o} + M_{x_1}\right) + A_{55}\left(\frac{u_1^a}{h} + w_1^o \frac{\pi}{\lambda}\right)$$

$$M_{y_o}' = \frac{\pi}{\lambda} M_{xy_1} + A_{44}\left(\frac{v_1^a}{h} + \beta_2\right)$$

$$N_{y_o}' = 0$$

$$Q_y' = \left(\frac{\pi}{\lambda}\right)^2 \left(M_{x_o} + \frac{1}{2} M_{x_2}\right) w_1^o - M_{x_1}\left(\frac{\pi}{\lambda}\right)^2 + A_{55}\left(\frac{u_1^a}{h} + w_1^o \frac{\pi}{\lambda}\right) + \frac{1}{2} N_{xy_2}\beta_2 \frac{\pi}{\lambda}$$

$$M_{y_1}' = \left(N_{y_o} - \frac{1}{2} N_{y_2}\right)\beta_2 + \frac{1}{2} N_{xy_2} w_1^o \frac{\pi}{\lambda} + \frac{2\pi}{\lambda} M_{xy_1} + A_{44}\left(\frac{v_1^a}{h} + \beta_2\right) - Q_y$$

where $\bar{D}_{ij} = -\frac{D_{ij}}{5b} \cdot \text{in.}$ $\quad \bar{B}_{ij} = -\frac{D_{ij}}{21\,b^2} \cdot \text{in.}^2$

and the superscript (') denotes differentiation with respect to y.

The stiffnesses of the plate are given by

$$A_{ij} = \int_{-h/2}^{h/2} C_{ij}\,dz \qquad D_{ij} = \int_{-h/2}^{h/2} C_{ij} z^2\,dz \qquad \text{(A6)}$$

where the C_{ij} are the stiffnesses in equation (8). Using the definition $\beta_2 = w_1^{o\prime}$ gives the following two differential equations, which complete the set of equations (14 equations with 14 unknowns) without squares of derivatives of the unknowns as required in the solution procedure (reference 11).

$$w_1^{o\prime} = \beta_2$$

$$\beta_2' = -\frac{v_1^{a\prime}}{h} - \left[\bar{D}_{22}\left(M_{y_o} - M_{y_1}\right) - D_{22} M_{y_1} + \left(\bar{D}_{22} D_{12} - D_{22}\bar{D}_{12}\right)\frac{u_1^a}{h}\frac{\pi}{\lambda} + \left(\bar{D}_{22}\bar{D}_{12} - D_{22}\bar{B}_{12}\right) \cdot \left(\frac{u_1^a}{h}\frac{\pi}{\lambda} + w_1^o\left(\frac{\pi}{\lambda}\right)^2\right)\right] \Big/ \left(D_{22}\bar{B}_{22} - \bar{D}_{22}^2\right) \qquad \text{(A7)}$$

The boundary conditions at $y = 0$ and $y = b$ are

$$u_2^o = u_1^a = 0,\ N_{y_o} = N_{y_2} = 0,\ w_1^o = 0,\ M_{y_o} = M_{y_1} = 0 \qquad \text{(A8)}$$

Three-dimensional flexibility theory

The displacements used in this theory are given by equations (4) as

$$\begin{aligned} u(x,y,z) &= u^o(x,y) + u^a(x,y)\frac{z}{h} + u^s(x,y)\sin\frac{\pi z}{h} \\ v(x,y,z) &= v^o(x,y) + v^a(x,y)\frac{z}{h} + v^s(x,y)\sin\frac{\pi z}{h} \\ w(x,y,z) &= w^o(x,y) + w^c(x,y)\cos\frac{\pi z}{h} \end{aligned} \qquad \text{(A9)}$$

Substitution of equations (4) into equations (7) and neglecting the nonlinear terms involving w^c gives the strain-displacement relations

$$\begin{aligned} \varepsilon_x &= u_{,x}^o + \frac{1}{2} w_{,x}^{o\,2} + u_{,x}^a \frac{z}{h} + u_{,x}^s \sin\frac{\pi z}{h} \\ \varepsilon_y &= v_{,y}^o + \frac{1}{2} w_{,y}^{o\,2} + v_{,y}^a \frac{z}{h} + v_{,y}^s \sin\frac{\pi z}{h} \\ \varepsilon_z &= -\frac{\pi}{h} w^c \sin\frac{\pi z}{h} \\ \gamma_{xy} &= u_{,y}^o + v_{,x}^o + w_{,x}^o w_{,y}^o + (u_{,y}^a + v_{,x}^a)\frac{z}{h} + (u_{,y}^s + v_{,x}^s)\sin\frac{\pi z}{h} \\ \gamma_{xz} &= w_{,x}^o + \frac{u^a}{h} + (w_{,x}^c + \frac{\pi}{h} u^s)\cos\frac{\pi z}{h} \\ \gamma_{yz} &= \frac{v^a}{h} + w_{,y}^o + (\frac{\pi}{h} v^s + w_{,y}^c)\cos\frac{\pi z}{h} \end{aligned} \qquad \text{(A10)}$$

The assumption that the displacements are sinusoidal along the length leads to

$$\begin{aligned} u^o &= -U\frac{x}{a} + u_2^o(y)\sin\frac{2\pi x}{\lambda} & v^o &= v_o^o(y) + v_2^o(y)\cos\frac{2\pi x}{\lambda} \\ u^a &= u_1^a(y)\cos\frac{\pi x}{\lambda} & v^a &= v_1^a(y)\sin\frac{\pi x}{\lambda} \\ u^s &= u_1^s(y)\cos\frac{\pi x}{\lambda} & v^s &= v_1^s(y)\sin\frac{\pi x}{\lambda} \\ & & w^o &= w_1^o(y)\sin\frac{\pi x}{\lambda} \\ & & w^c &= w_1^c(y)\sin\frac{\pi x}{\lambda} \end{aligned} \qquad \text{(A11)}$$

Stresses are determined from Hooke's law according to equation (8), and stress resultant forces and moments are determined by the following integrals through the thickness

$$\begin{aligned} N_{x_o} + N_{x_2}\cos\frac{2\pi x}{\lambda} &= \int_{-h/2}^{h/2} \sigma_x^o\,dz \\ N_{y_2}\sin\frac{2\pi x}{\lambda} &= \int_{-h/2}^{h/2} \sigma_y^o\,dz \\ N_{yz_1} &= \int_{-h/2}^{h/2} \tau_{yz}^o\,dz \\ N_{xz_1} &= \int_{-h/2}^{h/2} \tau_{xz}^o\,dz \\ N_{xy_2}\sin\frac{2\pi x}{\lambda} &= \int_{-h/2}^{h/2} \tau_{xy}^o\,dz \end{aligned} \qquad \text{(A12)}$$

$$M_{x_1} = \int_{-h/2}^{h/2} \left(\sigma_x^a\left(\frac{z}{h}\right) + \sigma_x^s \sin\frac{\pi z}{h}\right)\frac{z}{h}\,dz$$

$$M_{y_1} = \int_{-h/2}^{h/2} \left(\sigma_y^a\left(\frac{z}{h}\right) + \sigma_y^s \sin\frac{\pi z}{h}\right)\frac{z}{h}\,dz$$

$$M_{xy_1} = \int_{-h/2}^{h/2} \left(\tau_{xy}^a\left(\frac{z}{h}\right) + \tau_{xy}^s \sin\frac{\pi z}{h}\right)\frac{z}{h}\,dz$$

$$L_{x_1} = \int_{-h/2}^{h/2} \left(\sigma_x^a\left(\frac{z}{h}\right) + \sigma_x^s \sin\frac{\pi z}{h}\right)\sin\frac{\pi z}{h}\,dz$$

$$L_{y_1} = \int_{-h/2}^{h/2} \left(\sigma_y^a\left(\frac{z}{h}\right) + \sigma_y^s \sin\frac{\pi z}{h}\right)\sin\frac{\pi z}{h}\,dz$$

$$L_{z_1} = \int_{-h/2}^{h/2} \sigma_z^s \sin^2\frac{\pi z}{h}\,dz$$

$$L_{yz_1} = \int_{-h/2}^{h/2} \tau_{yz}^c \cos^2\frac{\pi z}{h}\,dz$$

$$L_{xz_1} = \int_{-h/2}^{h/2} \tau_{xz}^c \cos^2\frac{\pi z}{h}\,dz$$

$$L_{xy_1} = \int_{-h/2}^{h/2} \left(\tau_{xy}^a\left(\frac{z}{h}\right) + \tau_{xy}^s \sin\frac{\pi z}{h}\right)\sin\frac{\pi z}{h}\,dz$$

where the form of the stresses are

$$\sigma_x = \sigma_x^o + \sigma_x^a\frac{z}{h} + \sigma_x^s \sin\frac{\pi z}{h} \qquad \tau_{yz} = \tau_{yz}^o + \tau_{yz}^c \cos\frac{\pi z}{h}$$

$$\sigma_y = \sigma_y^o + \sigma_y^a\frac{z}{h} + \sigma_y^s \sin\frac{\pi z}{h} \qquad \tau_{xz} = \tau_{xz}^o + \tau_{xz}^c \cos\frac{\pi z}{h}$$

$$\sigma_z = \sigma_z^s \sin\frac{\pi z}{h} \qquad \tau_{xy} = \tau_{xy}^o + \tau_{xy}^a\frac{z}{h} + \tau_{xy}^s \sin\frac{\pi z}{h}$$

Substitution of the stresses and strains into the virtual work expression, equation (9), and performing the variation leads to the differential equations

$$u_2^{o\prime} = \frac{2\pi}{\lambda}v_2^o - \frac{1}{2}w_1^o\beta_1\frac{\pi}{\lambda} + \frac{N_{xy_2}}{A_{66}}$$

$$v_2^{o\prime} = \frac{1}{4}\beta_1^2 - \frac{A_{12}}{A_{22}}\left(u_2^o\frac{2\pi}{\lambda} + \frac{1}{4}w_1^{o2}\left(\frac{\pi}{\lambda}\right)^2\right) + \frac{N_{y_2}}{A_{22}}$$

$$\frac{u_1^{a\prime}}{h} = -\frac{v_1^a}{h}\frac{\pi}{\lambda} + \left(M_{xy_1} - \frac{J_{66}}{K_{66}}L_{xy_1}\right)\Big/\left(D_{66} - \frac{J_{66}^2}{K_{66}}\right) \qquad \text{(A13)}$$

$$\frac{v_1^{a\prime}}{h} = \left[\frac{L_{y_1}}{K_{22}} - \frac{M_{y_1}}{J_{22}} + \left(\frac{J_{12}}{K_{22}} - \frac{D_{12}}{J_{22}}\right)\frac{u_1^a}{h}\frac{\pi}{\lambda} + \left(\frac{K_{12}}{K_{22}} - \frac{J_{12}}{J_{22}}\right)u_1^s\frac{\pi}{\lambda}\right]\Big/\left(\frac{J_{22}}{K_{22}} - \frac{D_{22}}{J_{22}}\right)$$

$$u_1^{s\prime} = -\frac{\pi}{\lambda}v_1^s + \left(\frac{L_{xy_1}}{J_{66}} - \frac{M_{xy_1}}{D_{66}}\right)\Big/\left(\frac{K_{66}}{J_{66}} - \frac{J_{66}}{D_{66}}\right)$$

$$v_1^{s\prime} = \left[\frac{L_{y_1}}{J_{22}} - \frac{M_{y_1}}{D_{22}} + \left(\frac{J_{12}}{J_{22}} - \frac{D_{12}}{D_{22}}\right)\frac{u_1^a}{h}\frac{\pi}{\lambda} + \left(\frac{K_{12}}{J_{22}} - \frac{J_{12}}{D_{22}}\right)u_1^s\frac{\pi}{\lambda}\right]\Big/\left(\frac{K_{22}}{J_{22}} - \frac{J_{22}}{D_{22}}\right)$$

$$w_1^{o\prime} = -\frac{v_1^a}{h} + \left(\frac{N_{yz_1}}{H_{44}} - \frac{L_{yz_1}}{I_{44}}\right)\Big/\left(\frac{A_{44}}{H_{44}} - \frac{H_{44}}{I_{44}}\right)$$

$$w_1^{c\prime} = -\frac{\pi}{h}v_1^s - \left(\frac{N_{yz_1}}{A_{44}} - \frac{L_{yz_1}}{H_{44}}\right)\Big/\left(\frac{I_{44}}{H_{44}} - \frac{H_{44}}{A_{44}}\right)$$

$$N_{xy_2}' = \frac{2\pi}{\lambda}N_{x_2}$$

$$N_{y_2}' = -\frac{2\pi}{\lambda}N_{xy_2}$$

$$M_{xy_1}' = N_{xz_1} - M_{x_1}\frac{\pi}{\lambda}$$

$$M_{y_1}' = N_{yz_1} + M_{xy_1}\frac{\pi}{\lambda}$$

$$L_{xy_1}' = L_{xz_1}\frac{\pi}{h} - L_{x_1}\frac{\pi}{\lambda}$$

$$L_{yz_1}' = L_{xz_1}\frac{\pi}{\lambda} - L_{z_1}\frac{\pi}{h}$$

$$L_{y_1}' = L_{yz_1}\frac{\pi}{h} + L_{xy_1}\frac{\pi}{\lambda}$$

$$Q' = \left(N_{x_o} + \frac{N_{x_2}}{2}\right)w_1^o\left(\frac{\pi}{\lambda}\right)^2 + \frac{1}{2}N_{xy_2}\beta_1\frac{\pi}{\lambda} + N_{xz_1}\frac{\pi}{\lambda}$$

The stiffnesses of the plate are given by

$$A_{ij} = \int_{-h/2}^{h/2} C_{ij}\,dz \qquad H_{ij} = \int_{-h/2}^{h/2} C_{ij}\cos\frac{\pi z}{h}\,dz$$

$$K_{ij} = \int_{-h/2}^{h/2} C_{ij}\sin^2\frac{\pi z}{h}\,dz \qquad D_{ij} = \int_{-h/2}^{h/2} C_{ij}z^2\,dz \qquad \text{(A14)}$$

$$J_{ij} = \int_{-h/2}^{h/2} C_{ij}z\sin\frac{\pi z}{h}\,dz \qquad I_{ij} = \int_{-h/2}^{h/2} C_{ij}\cos^2\frac{\pi z}{h}\,dz$$

where the C_{ij} are the stiffnesses in equation (8). The definition $\beta_1 = w_1^{o\prime}$ is not used in this theory due to differences in the formulation of the theories. Instead, the following definition of β_1 is used

$$\beta_1 = \left\{-\frac{v_1^a}{h} + \left[\frac{1}{H_{44}}\left(Q - \frac{1}{2}\frac{\pi}{\lambda}N_{xy_2}w_1^o\right) - \frac{L_{yz_1}}{I_{44}}\right]\Big/\left(\frac{A_{44}}{H_{44}} - \frac{H_{44}}{I_{44}}\right)\right\} \cdot \qquad \text{(A15)}$$
$$1\Big/\left[1 + \frac{1}{H_{44}}\frac{N_{y_2}}{2}\Big/\left(\frac{A_{44}}{H_{44}} - \frac{H_{44}}{I_{44}}\right)\right]$$

which results in the completely defined set of equations (16 equations with 16 unknowns) without squares of derivatives of the unknowns as required in the solution procedure.

The boundary conditions used at y = 0 and y = b are

$$u_2^o = u_1^a = u_1^s = 0,\ N_{y_o} = N_{y_2} = 0,\ w_1^o = w_1^c = 0,\ M_{y_1} = L_{y_1} = 0 \qquad \text{(A16)}$$

ACKNOWLEDGEMENTS

The authors would like to gratefully acknowledge the computer support given by Nancy Jane C. Bains at NASA Langley Research Center and Dr. James Fulton at Hampton University.

References

1. Stein, M.: Nonlinear Theory for Laminated and Thick Plates and Shells Including the Effects of Transverse Shearing. AIAA Journal, Vol. 24, September 1986, pp. 1537-1544.

2. Stein, M.; and Bains, N. J. C.: Postbuckling Behavior of Longitudinally Compressed Orthotropic Plates with Three-Dimensional Flexibility. AIAA Paper No. 86-0976 CP, May 1986.

3. Stein, M.: Postbuckling of Orthotropic Composite Plates Loaded in Compression. AIAA Journal, Vol. 21, December 1983, pp. 1729-1735.

4. Mindlin, R. D.: Influence of Rotatory Inertia and Shear on Flexural Motions of Isotropic, Elastic Plates. Journal of Applied Mechanics, Vol. 18, 1951, pp. 31-38.

5. Librescu, L.: Elastostatics and Kinetics of Anisotropic and Heterogeneous Shell-Type Structures. Noordhoff, Leyden, German Democratic Republic, 1975.

6. Murthy, M. V. V.: An Improved Transverse Shear Deformation Theory for Laminated Anisotropic Plates. NASA Technical Paper 1903, November 1981.

7. Phan, N. D.; and Reddy, J. N.: Analysis of Laminated Composite Plates Using a Higher-Order Shear Deformation Theory. International Journal for Numerical Methods in Engineering, Vol. 21, 1985, pp. 2201-2219.

8. Stein M.; Sydow, P. D.; and Librescu, L.: Postbuckling of Long Thick Plates in Compression Including Higher Order Transverse Shearing Effects. Advances in the Theory of Plates and Shells, edited by G. Z. Voyiadjis and D. Karamanlidis, Elsevier, 1990, pp. 63-86.

9. Librescu, L.; and Stein, M.: A Geometrically Nonlinear Theory of Shear Deformable Laminated Composite Plates and its Use in the Postbuckling Analysis. Proceedings of the International Congress of the Aeronautical Sciences, Vol. 1, Jerusalem, Israel, August 28-September 2, 1988, pp. 349-359.

10. Reissner, E.: The Effect of Transverse Shear Deformation on the Bending of Elastic Plates. Journal of Applied Mechanics, Vol. 12, No. 1, 1945, pp. A-69 to A-77.

11. Lentini, M. and Pereyra, V.: An Adaptive Finite Difference Solver for Nonlinear Two-Point Boundary Problems with Mild Boundary Layers. SIAM Journal of Numerical Analysis, Vol. 14, No.1, March 1977.

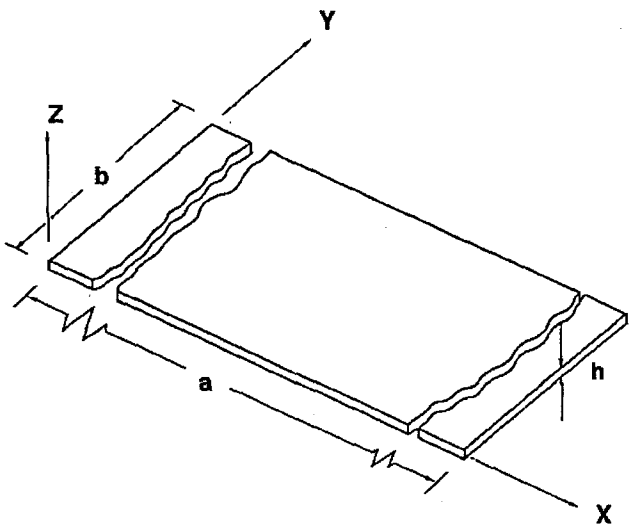

Fig. 1 Plate Geometry.

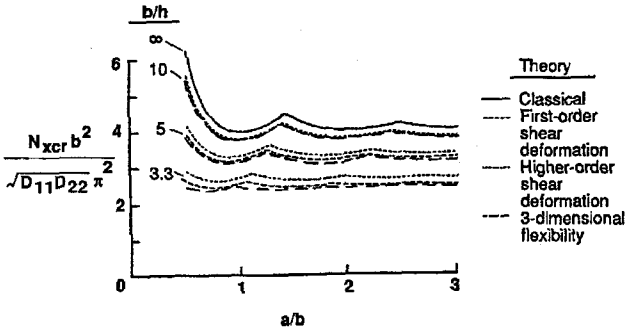

Fig. 2 Critical axial stress resultant, N_{xcr}, versus plate length-to-width ratio, a/b, for different width-to-thickness ratios, b/h, and different theories for aluminum plates of finite length.

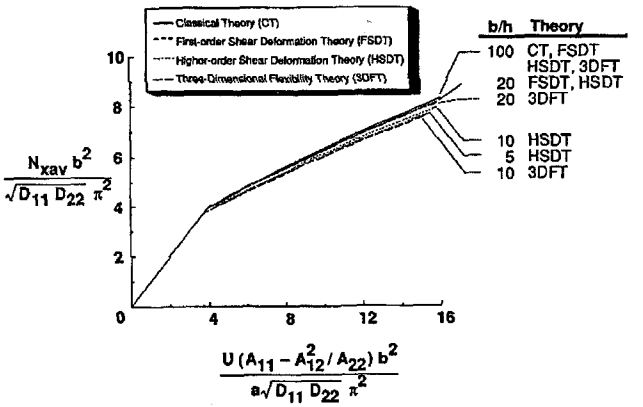

Fig. 3a Average axial stress resultant, N_{xav}, versus applied end-shortening, U, for different width-to-thickness ratios, b/h, and different theories for aluminum plates of infinite length where U/a is finite.

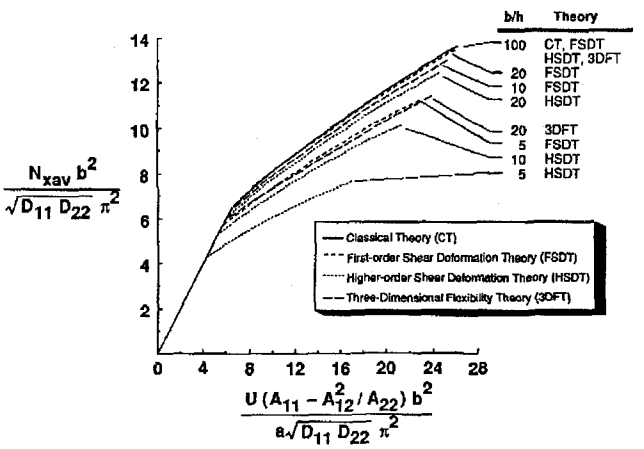

Fig. 3b Average axial stress resultant, N_{xav}, versus applied end-shortening, U, for different width-to-thickness ratios, b/h, and different theories for ±45 ° composite plates of infinite length where U/a is finite.

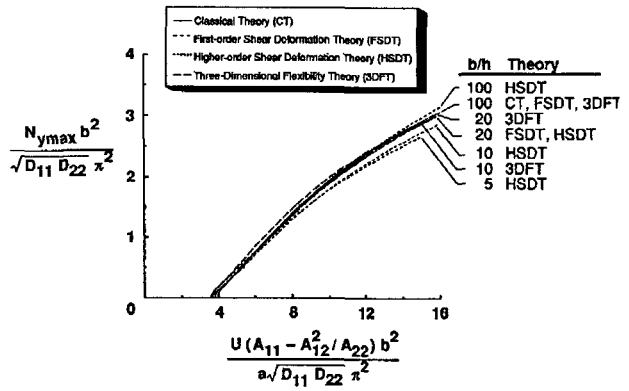

Fig. 4a Maximum transverse stress resultant, N_{ymax}, versus applied end-shortening, U, for different width-to-thickness ratios, b/h, and different theories for aluminum plates of infinite length where U/a is finite.

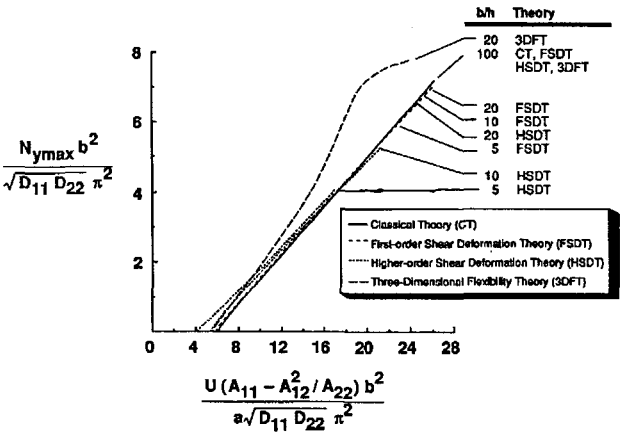

Fig. 4b Maximum transverse stress resultant, N_{ymax}, versus applied end-shortening, U, for different width-to-thickness ratios, b/h, and different theories for ±45 ° composite plates of infinite length where U/a is finite.

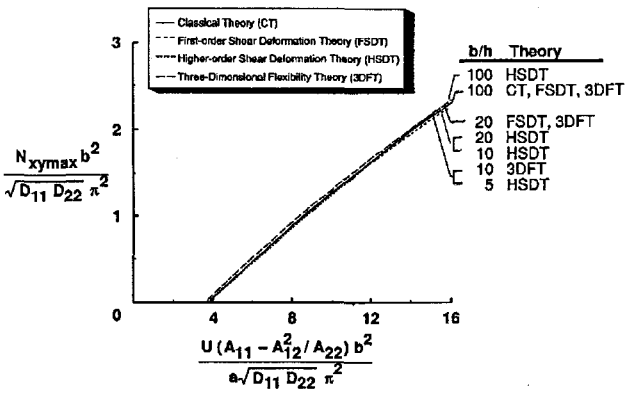

Fig. 5a Maximum shear stress resultant, N_{xymax}, versus applied end-shortening, U, for different width-to-thickness ratios, b/h, and different theories for aluminum plates of infinite length where U/a is finite.

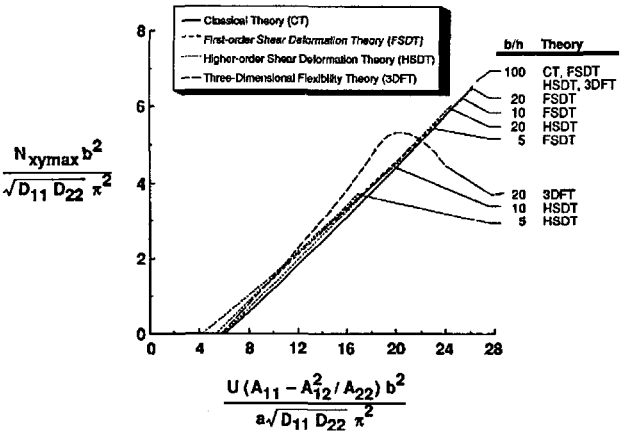

Fig. 5b Maximum shear stress resultant, N_{xymax}, versus applied end-shortening, U, for different width-to-thickness ratios, b/h, and different theories for ±45 ° composite plates of infinite length where U/a is finite.

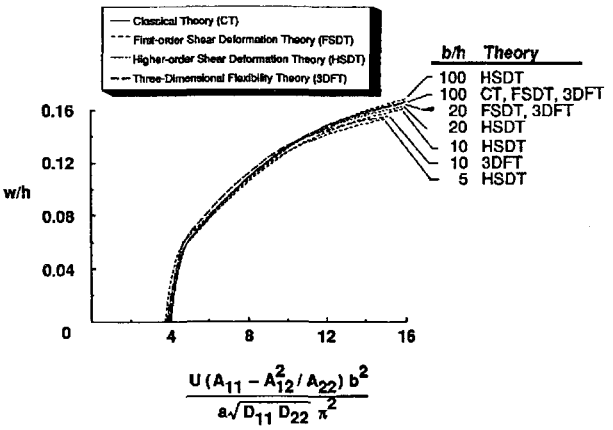

Fig. 6a Out-of-plane displacement, w, versus applied end-shortening, U, for different width-to-thickness ratios, b/h, and different theories for aluminum plates of infinite length where U/a is finite.

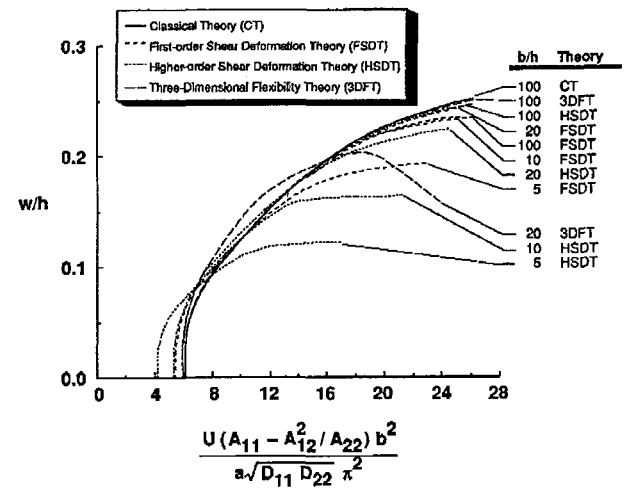

Fig. 6b Out-of-plane displacement, w, versus applied end-shortening, U, for different width-to-thickness ratios, b/h, and different theories for ±45 ° composite plates of infinite length where U/a is finite.